Tellus (2007), 59B, 22–38
Printed in Singapore. All rights reserved

TELLUS

OH and halogen atom influence on the variability of non-methane hydrocarbons in the Antarctic Boundary Layer

By KATIE A. READ[1]*, ALASTAIR C. LEWIS[1], RHIAN A. SALMON[2], ANNA E. JONES[2] and STÉPHANE BAUGUITTE[2], [1]*Department of Chemistry, University of York, Heslington, York YO19 4RR, UK;* [2]*British Antarctic Survey, Madingley Road, High Cross, Cambridge, UK*

(Manuscript received 21 December 2005; in final form 4 September 2006)

ABSTRACT

Measurements of C_2–C_8 non-methane hydrocarbons (NMHCs) have been made *in situ* at Halley Base, Antarctica (75°35′S, 26°19′W) from February 2004 to February 2005 as part of the Chemistry of the Antarctic Boundary Layer and the Interface with Snow (CHABLIS) experiment. The data show long- and short-term variabilities in NMHCs controlled by the seasonal and geographic dependence of emissions and variation in atmospheric removal rates and pathways. Ethane, propane, *iso*-butane, *n*-butane and acetylene abundances followed a general OH-dependent sinusoidal seasonal cycle. The yearly averages were 186, 31, 3.2, 4.9 and 19 pptV, respectively, lower than those which were reported in some previous studies. Superimposed on a seasonal cycle was shorter-term variability that could be attributed to both synoptic airmass variability and localized loss processes due to other radical species. Hydrocarbon variability during periods of hour-to-day-long surface O_3 depletion in late winter/early spring indicated active halogen atom chemistry estimated to be in the range 1.7×10^3–3.4×10^4 atom cm^{-3} for Cl and 4.8×10^6–9.6×10^7 atom cm^{-3} for Br. Longer-term negative deviations from sinusoidal behaviour in the late August were indicative of NMHC reaction with a persistent [Cl] of 2.3×10^3 atom cm^{-3}. Maximum ethene and propene of 157 and 179 pptV, respectively, were observed in the late February/early March, consistent with increased oceanic biogenic emissions; however, their presence was significant year-round (June–August concentrations of 17.1 ± 18.3 and 7.9 ± 20.0 pptV, respectively).

1. Introduction

Although seen as being a more natural representation of background conditions compared to the Arctic atmosphere, the less-accessible Antarctic troposphere has received relatively little scientific attention. Atmospheric studies have focused mainly on stratospherically important or long-lived radiatively active gases rather than tropospheric species. Surface ozone (O_3) has been measured inland at the South Pole, at Neumayer, and at Syowa (Schnell et al., 1991; Murayama et al., 1992; Wessel et al., 1998); however, prior to March 2003, only one data set existed for Halley and this was obtained in 1958 (Royal Society, 1962).

The chemistry of the Antarctic Boundary Layer (which is often shallow and strongly stratified) is influenced strongly by snow–air interactions (Dominé and Shepson, 2002). A number of field experiments have been carried out to study this, including both the Photochemical Experiment at Neumayer (PEAN'99) (Jacobi et al., 2000; Fischer et al., 2002), and the Polar Sunrise Experiments (PSE): ALERT 2000 and Summit 2000 (Bottenheim et al., 2002b). These and other short-term experiments have included investigations into the snow pack production of trace species, for example, of NO_x (Jones et al., 2000), H_2O_2, CH_3OOH and HCHO (Sumner and Shepson, 1999; Riedel et al., 2000; Jacobi et al., 2002) and HONO (Zhou et al., 2001). In the Antarctic Boundary Layer itself, however, there are limited long-term measurements of these species, and indeed of other reactive chemicals.

Atmospheric experiments with a focus on urban environments have shown that pollution sources dominate the changing levels of all non-methane hydrocarbon (NMHC) species (Hopkins et al., 2005; Durana et al., 2006). In remote areas such as the Antarctic Boundary Layer, the sources are much smaller and so NMHC variability is highly dependent on the oxidizing capacity of the atmosphere (Kanakidou et al., 1991; Bloss et al., 2005). The changing distribution of longer-lived NMHC in more remote regions can provide valuable information on prevailing oxidant climatology and long-range meteorological transport. Shorter-lived alkenes may influence local free radical

*Corresponding author
e-mail: km519@york.ac.uk
DOI: 10.1111/j.1600-0889.2006.00227.x

production and loss and therefore their measurement will aid us in our understanding of these processes.

In most remote atmospheres, the seasonal cycle of alkanes is known to be highly dependent on their atmospheric removal rate by the hydroxyl radical (Jobson et al., 1994b; Goldstein et al., 1995; Rudolph, 1995; Sharma et al., 2000). In the Antarctic troposphere, this has only been studied by collecting a relatively small number of spot samples (usually via canister sampling), which are then returned to laboratories for analysis (Rudolph et al., 1989; Rudolph et al., 1992; Clarkson et al., 1997). In addition, the remoteness of Antarctic stations has resulted in only limited measurements collected during the winter period and therefore has achieved a poor temporal coverage (perhaps only one sample per day). Whilst the seasonal variability of these species has been established in previous studies, shorter-term variability detectable only with high-time-resolution measurements and which carries most information on the oxidizing environment has been underexploited. Recent developments of automatic techniques and improvements in instrumental detection limits have allowed more opportunity for advancement in this area (Yamamoto et al., 1998; Wang et al., 2000; Hopkins et al., 2002; Wevill and Carpenter, 2004). In particular, full automation allows the uninterrupted study of photochemical processes during the extreme Antarctic conditions, such as the transitions between continuous sunlight in austral summer and continuous darkness in austral winter. During these transitions when $j\mathrm{O}^1\mathrm{D}$ and hence OH concentrations will be low, variability in NMHC mixing ratios results either from large-scale meteorological transport events, or may indicate the presence of other chemical activity relating to halogen atoms such as chlorine and bromine (Jobson et al., 1994a). These radicals lead to increased rates of removal of NMHCs and of CH_4, a radiatively-active greenhouse gas.

The aim of the Chemistry of the Antarctic Boundary Layer and the Interface with Snow (CHABLIS) experiment was to investigate the photochemistry of the Antarctic region and to determine the factors that are controlling it. To achieve this, more frequent NMHC measurements compared to previous studies (Rudolph et al., 1989; Clarkson et al., 1997; Gros et al., 1998) have been collected in order to reduce uncertainties on monthly means and to allow investigation into their seasonal and short-term variability. This paper introduces those measurements of C_2–C_8 NMHCs made at Halley, Antarctica between February 2004 and February 2005.

2. Site description

Halley research station is situated at the farthest South of all the British Antarctic Survey (BAS) bases at 75°35′S, 26°19′W. It is built on the floating Brunt Ice Shelf, 15 km from the coast of the Weddell Sea. Measurements were made at the newly commissioned **C**lean **A**ir **S**ector **Lab**oratory (CASLab) positioned 1 km south-east of the main station in the Clean Air Sector

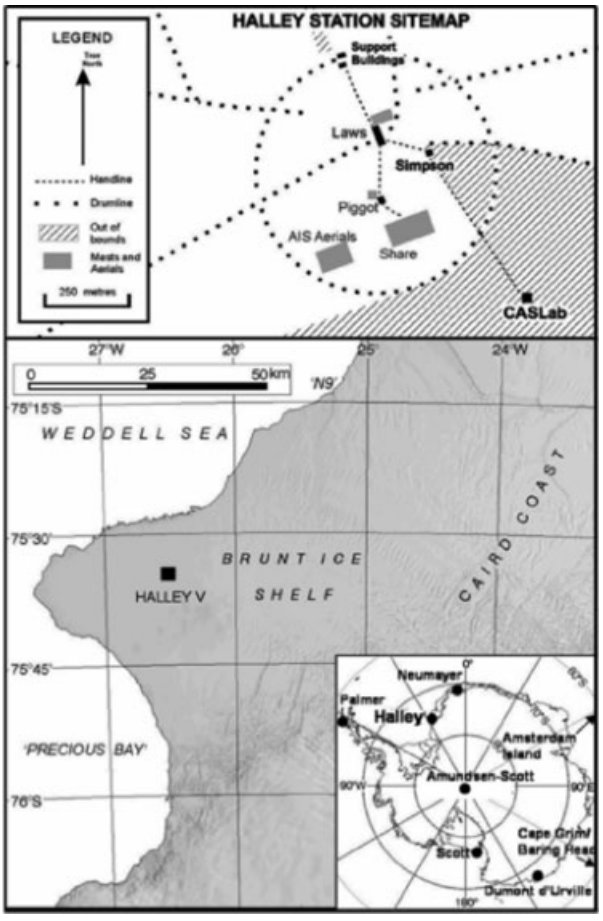

Fig. 1. Halley Station site plan showing the positions of the Clean Air Sector and CASLab. Inset map of Antarctica highlighting positions of bases.

(Fig. 1). Prevailing winds to Halley are from the East and so air approaches the measurement site from across the ice shelf plateau. This means that the CASLab is rarely influenced by the station (North of site) and any generators. Aircraft avoided the Clean Air Sector according to protocol and routine access to the CASLab is by foot or by ski. Except for a small amount produced by the base, there are no local sources of anthropogenic pollution, and therefore NMHCs are dominated by long-range transport processes and oceanic or snow pack emissions.

3. Experimental

A heated inlet positioned at a height of 8 m was connected to a low residence time (<1 s), 10-cm-diameter stainless steel manifold from which almost all CASLab instruments were subsampled. 750-ml air samples were taken using a pump pulling air through the Programmable Temperature Vaporisation Injection-Gas Chromatograph-Flame Ionization Detection (PTV-GC-FID) system at a flow rate of 50 ml min^{-1} for 15 min every 75 min.

Table 1. Measurements made during CHABLIS which are discussed within this publication

Species measured	Analytical technique	Temporal resolution	Detection limit	Measurement uncertainty
NMHC	Gas Chromatography/ Flame Ionization Detection	60 min	2–5 pptv for C_2–C_5 10 pptv for C_6–C_8	<10 pptv[a]
Black carbon	Aethalometer	5 min averaged to 2 h	5 ng m^{-3} (reduced to 0.5 ng m^{-3} if averaged over a day)	5 ng m^{-3}
O_3	2B Technologies UV analyser	10 s averaged to 1 min	1.5 ppbv	1.5 ppbv (1σ)/ 2%
CO	Aerolaser fast response resonance fluorescence	10 s, 30 s	1.5 ppbv	0.7 ppbv (1σ), 0.2 ppbv (1σ)

[a]See Experimental section for discussion of this measurement uncertainty.

The NMHCs were pre-concentrated on to a carbon adsorbent trap at –25°C. A Valco (Supelco, UK) valve allowed the transfer of sample to a 50 m 0.53 mm i.d. Al_2O_3 PLOT column in a helium carrier flowing at 21 ml min^{-1} and the trap was subsequently heated to 400°C. After 4 min at 42°C, the chromatographic oven program increased the temperature of the oven at 6°C min^{-1} to 200°C where it was held for 21 min. Chromatographic analyses of NMHC can be done much more rapidly using faster ramp rates and shorter running times; however, it was important to keep the power consumption low and although the analysis time was lengthened, this was of lesser importance on such a long-term study. An autosampler upstream of the GC was in place for alternating air samples, calibrations and blanks; the latter of which were initially performed weekly and then fortnightly once instrumental performance had been established. Measurement uncertainty in Gas Chromatography arises from a combination of imprecision in sample volume, calibration uncertainty, and peak integration uncertainty. The samples were performed using the same set-up as the calibration and so errors in sample volume were minimal, at <1%. Calibrations were performed using a 28 hydrocarbon component in nitrogen standard at the pptV level in addition to a ppbV standard and varied by <10% over the course of the year with no systematic change in response. Errors such as those within the calibration standard remained constant since a linear regression was assumed for the calibration. The main precision errors arose from the peak integration. Knowledge and understanding of the detector response leads to the assumption that a power relationship relates the concentration (or peak size) to the error. Therefore, when peak size becomes comparable to the detector noise, the relative error approaches 100% but for larger peaks the relative error was closer to 1%. These relative errors relate to very small absolute errors, which were calculated for each peak individually and which hardly ever approached 10 pptv (quoted upper limit for uncertainty). The detection limits were 2–5 pptV for C_2–C_5 NMHCs and 10 pptV for C_6–C_8 NMHCs. Data were returned to the UK weekly via an ftp (file transfer protocol) site and a total of 7800 chromatograms were analysed to produce this data set. Table 1 details the measurement techniques used to obtain ozone, carbon monoxide, and black carbon data together with the temporal resolution, detection limits and measurement uncertainties of these and the NMHC measurements.

4. Results and Discussion

4.1. Comparison with other studies

Of all the NMHCs, the most extensively measured in the Southern Hemisphere are ethane and propane largely because they are stable in canisters and are in the highest concentrations. During this year-long campaign, their respective averages were 186 ± 74 and 31 ± 21 pptV, up to a factor of around 2 lower than those which were previously reported (Bonsang et al., 1990; Rudolph et al., 1992; Clarkson et al., 1997). Table 2 details a varied selection of previously reported values, for both summer (~January–February in black) and winter (~July–August in italics) together with the date and latitude where they were obtained.

Results from Cape Grim, located at 40°7′S, 144°7′E, were the most recently published *in situ* measurements and the most similar in magnitude, although the average values calculated from the research stations, Scott Base in the Antarctica (77°51′S, 166°45′E) and Baring Head in New Zealand (41°24′S, 174°52′E), were also comparable. Scott Base is also a coastal site but located on the other side of Antarctica in the Pacific sector (see Fig. 1) and so agreement suggests a consistent value for light alkanes throughout coastal Antarctica. Individual summer and winter values were not available for the site closest to Halley, German base Georg von Neumayer (70°36′ S, 8°22′ W), but average annual values for ethane, propane, *n*-butane and *iso*-pentane of 380 ± 8, 84 ± 4, 50 ± 4 and 15 ± 2 pptV (Rudolph et al., 1992), respectively, were somewhat higher than those measured during CHABLIS and previous comparisons have alluded to there being some impact from less-remote sources such as southern Africa or South America (Clarkson et al., 1997).

Table 2. Summary of mean NMHC measurements obtained in the Marine Boundary Layer of the Southern Hemisphere from the literature. Summer in normal font, and winter in italics. All in pptv. (a) = automatic, (m) = manual. Measurements reported from Georg Von Neumayer are rough values read from published plots. To calculate the Halley mean values in this study actual measurements were used even if they fell below the detection limit

Location	Date and reference	C_2H_6	C_3H_8	C_2H_4	C_3H_6	C_2H_2	i-C_4H_{10}	n-C_4H_{10}	i-C_5H_{12}	n-C_5H_{12}
Scott Base (m)/Baring Head (a)	Jan ′91–′96	200 ± 6	25 ± 3							
77°51′S / 41° 24′S	(Clarkson et al. 1997)									
Ship measurements (m)	Jan ′91–′96	291 ± 76	61± 53			48 ± 35	26	51		
43°S–77°S	(Gros et al. 1998)									
Cape Grim, Tasmania (a)	Jan–Feb ′99	142	8.8				5.6	9.9	2.3	3.2
40°7′S, 144°7′E	(Lewis et al. 2001)									
Georg von Neumayer	Summer ′82–′85	∼300	∼50	∼20	∼100	∼8.0				
70°36′S, 8°22′W (from graphs)	(Rudolph et al. 1989)									
70°36′S, 8°22′W (from graphs)	Dec ′03–Feb ′04	126 ± 39	16 ± 14	15 ± 18	10 ± 32	1.0 ± 7.2	0.7 ± 3.2	1.0 ± 4.6		
Scott Base (m)/Baring Head (a)	*Jul ′91–′96*	*356 ± 7*	*60 ± 4*							
77°51′S / 41° 24′S	*(Clarkson et al. 1997)*									
Georg von Neumayer	*Winter ′82–′85*	*∼450*	*∼100*	*∼30*	*∼250*	*∼20*				
70°36′S, 8°22′W (from graphs)	*(Rudolph et al. 1989)*									
Halley (a) 75°35′S, 26°19′W	*Jun–Aug ′04*	*276 ± 33*	*49 ± 18*	*17 ± 18*	*9.3 ± 11*	*42 ± 14*	*7.8 ± 6.5*	*13 ± 7.0*		

Compounds such as *iso*-butane, *n*-butane, *n*-pentane and acetylene which are indicative of relatively recent long-range transport of pollution were mostly absent in the summer months at Halley, and thus providing the assurance that the concentrations measured were not influenced by anthropogenic emissions, but are truly 'background' signatures.

4.2. Seasonal variation of alkanes

Ethane and propane showed a significant seasonal cycle with a January–February minimum and July–August maximum (Fig. 2) corresponding to a seasonally-dependent OH concentration (Kanakidou et al., 1991, Bloss et al., 2005). As concentrations increased, the instrument signal-to-noise ratio (S/N) improved, and there was generally less apparent short-term variability. *Iso*-butane, *n*-butane and acetylene also showed a similar seasonal cycle to the lower alkanes with increasing values in austral winter (Figs. 3 and 4). *Iso*- and *n*-butane mixing ratios were generally close to the instrumental detection limit, and showed high variability throughout the year with average concentrations of 3 ± 7 and 5 ± 17 pptV, for *iso*- and *n*-butane, respectively. During CHABLIS, acetylene reached maximum values of 107 pptV in winter, which was higher than previously reported measurements (Rudolph et al., 1989). Its main global source is engine exhausts (PORG, 1993), although a source from biomass burning is thought to be significant in the Southern Hemisphere (Rudolph et al., 1992). The yearly average and magnitude of the summer-to-winter increase were in agreement with those of Kaspers et al., (2004) who used Antarctic firn measurements to model atmospheric concentrations for this species. Rudolph et al., (1992) saw a 65 ± 12% rise attributed to biomass burning influences but considering the black carbon data which showed no obvious increases (Fig. 4), an influence from this source was not thought to be significant in this study. Acetylene has also been known to have a weak source from oceans but the flux is at least a factor of 2 lower than those of ethene and propene which were observed in relatively lower concentrations (Kanakidou et al., 1988; Ratte et al., 1998). The origin of the observed acetylene therefore remains under discussion.

A sinusoidal fit was applied to the ethane and propane, which allowed comparison with other NMHC data sets (Fig. 2). The increase from an average of 95 ± 34 pptV (1σ) for ethane in January to 283 ± 44 pptV (1σ) in August had a calculated amplitude of 94 ± 55 pptV but the fit suggested a value of 108 pptV. This was in good agreement with that seen by Clarkson et al., (1997) who reported a 120-pptV change at Scott Base and also with measurements of ethane made at the South Pole (Khalil and Rasmussen, 1986) and at Georg Von Neumayer (Rudolph et al., 1989; Rudolph et al., 1992) (Table 3). The maxima in both ethane and propane appear to vary between measurement

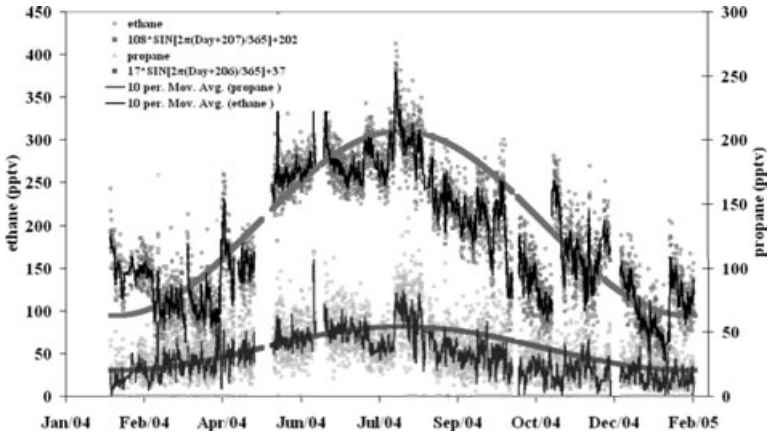

Fig. 2. Time-series of ethane and propane measured *in situ* at Halley during 2004–2005 with sinusoidal fits applied.

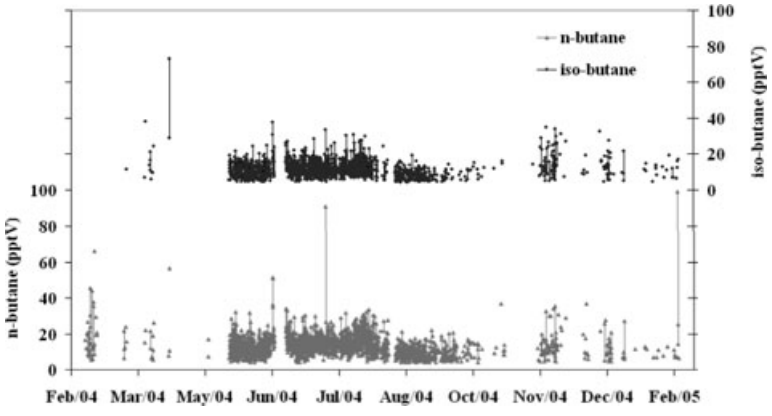

Fig. 3. Time-series of *iso*- and *n*-butane measured *in situ* at Halley during 2004–2005.

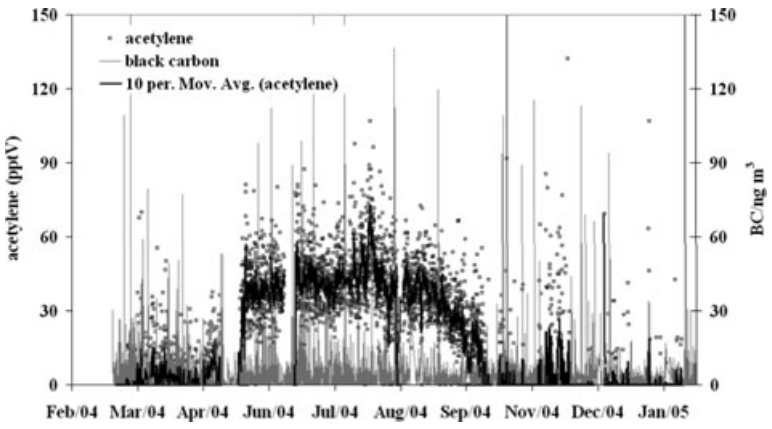

Fig. 4. Time-series of acetylene and black carbon measured *in situ* at Halley during 2004–2005.

sites, occurring in September rather than in August in most of the previous data sets published (Rudolph et al., 1989; Rudolph et al., 1992; Gros et al., 1998) and as late as October for the South Pole data set (Khalil and Rasmussen, 1986). This delay in seasonal maximum has previously been attributed to increased sources for this species from biomass burning, which is at a maximum in countries such as South America (August–October) and Southern tropical Africa (June–October) at this time of the year (Rudolph et al., 1992; Andreae and Merlet, 2001).

4.3. Impact of airmass origin on the sinusoidal fits

In line with Halley being situated farther South than most other reported studies (Rudolph et al., 1989; Bonsang et al., 1990; Rudolph et al., 1992; Lewis et al., 2001) and away from major anthropogenic influences, the small-scale variability was also significantly smaller than that of previous data sets for this region of the atmosphere. The main day-to-week time-scale deviations from the sine curve, clearly visible as a result of the generally

Table 3. Sinusoidal analysis comparison for ethane and propane

Ethane Site	Mean	Amplitude	Maximum	Minimum	Reference
Baring Head	296	138	September	March (JD88)	(Clarkson et al. 1997)
Scott Base	288	120	September	March (JD70)	(Clarkson et al. 1997)
South Pole		95	October	January	(Khalil and Rasmussen 1986)
Georg von Neumayer	380	88	August/September	January	(Rudolph et al. 1989; Rudolph et al. 1992)
Halley, this study	185	108	August	January	–
Propane					
Site	Mean	Amplitude	Maximum	Minimum	Reference
Baring Head	38	24	September	March (JD66)	(Clarkson et al. 1997)
Scott Base	43	23	August/September	January (JD30)	(Clarkson et al. 1997)
Georg von Neumayer	85	20	August/September	January-March	(Rudolph et al. 1989; Rudolph et al. 1992)
Halley, this study	31	17	August	January	-

small variability on low absolute levels, arise from changes in the airmass origins received by the site.

The predominant wind direction experienced by the Halley site is from the East, a likely effect of winds with a mainly downslope component crossing the Antarctic terrain height contours at angles between 30° and 60° (Kottmeier and Fay, 1998). However, if we consider the eight-day-back trajectories for these airmasses, we can obtain further information with respect to the path the air has taken previously. The European Centre for Medium range Weather Forecasting (ECMWF) calculated trajectories for the Antarctic use wind analyses but care must be taken with their reliability as they are based on fewer surface and upper air meteorological observations than in other areas of the world (ECMWF, 1995). Having said that, following the work of Kottmeier and Fay, (1998), the air received by Antarctica and the Halley site can be characterized into four main airmass types based on previous eight-day-back trajectory analyses. This 'Halley climatology' was in good agreement with the small number of trajectories calculated specifically for the 2004–2005 experiment. Fig. 5 shows typical back trajectories from this study to illustrate an example for each type.

(i) Directly advected airmasses from oceanic sectors (Oceanic).

(ii) Coastal airmasses arising from low-pressure cyclonic systems passing offshore and flowing marine air on to the margin ice sheet and sustained for periods of a few hours to a few days (Coastal).

(iii) Continental air from inland Antarctic plateau occurring as a result of katabatic winds which are initiated by horizontal density gradients and the slope between cold air at the surface and relatively warmer upper air (Continental).

(iv) Air from the Antarctic Peninsula region (Peninsula).

Airmasses with North/north-easterly back trajectories are generally advected from surrounding oceanic and continental regions (Fig. 5a). Northerly air is hardly ever observed but the back trajectories for these airmasses tend to travel closer to the surface (<3 km height) and are therefore subjected to more influence from boundary layer and low tropospheric chemistry.

Synoptic-scale low-pressure cyclones move eastwards around the continent, an effect of the circumpolar trough over Antarctica, and give rise to air arriving at the site from the south-easterly direction. These airmasses, which have some continental background, tend not to penetrate far inland Antarctica but can generate very strong winds along the coast and at Halley (Fig. 5b). Air originating from the South (although rarely from farther South than 75 °S) has almost always travelled over the Antarctic continent, descending over the marginal plateau and the slope region (Fig. 5c). Westerly air is less frequently received by the site but when it is observed the corresponding back trajectories originate in the direction of the Antarctic Peninsula, and show that the air crosses the Bellingshausen Sea *en route* to Halley (Fig. 5d).

The probability that within the past eight days the air sampled at Halley had any contact with ice-free continents was very small and this was generally insufficient time for a trajectory to be confidently assigned to a land origin. The sources for hydrocarbons in this region are poorly defined and there was no specific airmass type/origin which systematically resulted in higher concentrations when compared to another (Fig. 6). Having said that, it is clear that the observed changes in concentration and subsequent deviations from the sinusoidal trend do reflect bulk changes in the airmass nonetheless (inset in Fig. 6).

4.4. Smaller scale features superimposed on the seasonal cycles

During this experiment, a key advantage to collect data *in situ* and at a higher temporal resolution when compared to previous studies, was that fine scale events were captured (Rudolph et al., 1992; Touaty et al., 1996; Swanson et al., 2003). This

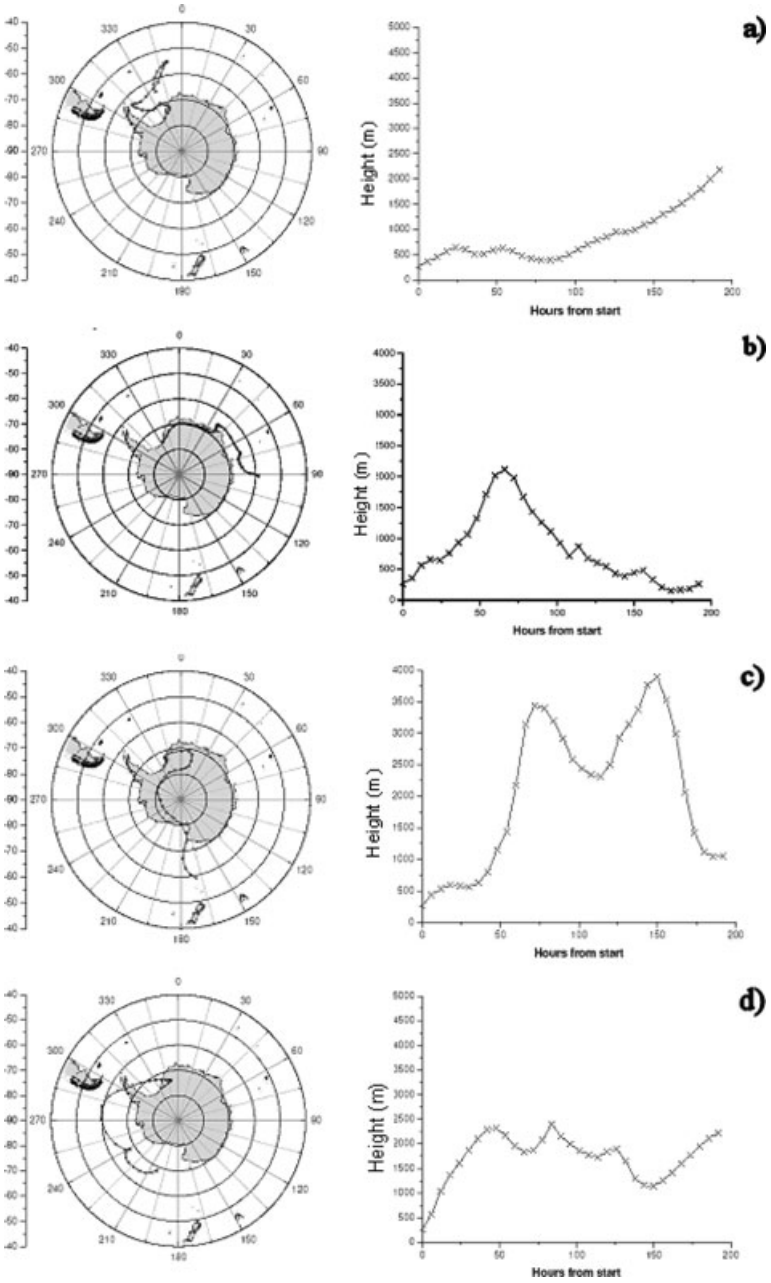

Fig. 5. Typical airmass plots for four types of conditions. From top: (a) Oceanic, (b) Coastal, (c) Continental, and (d) Peninsula. See the text for detail.

has allowed us to observe additional deviations from the annual OH-driven cycle associated with individual short-term chemical process changes, in addition to the bulk airmass classifications described previously.

4.4.1. NMHC behaviour during surface ozone depletion events. Similar to previous observations in both Antarctica and the Arctic, during early spring, tropospheric O_3 concentrations at Halley were observed to rapidly decrease and stay low for periods from a few hours to 6 days (Jobson et al., 1994a; Ariya et al., 1999; Jones et al., 2006). One such event occurred on the 2nd of September and is illustrated in Fig. 7, when the concentration of O_3 dropped by 23 ppbV. NMHC concentrations were also seen to vary during this time with the decreasing acetylene mixing ratio correlated to the O_3 mixing ratio, whilst the benzene and CO mixing ratios remained in relatively constant levels throughout (Fig. 7). On first inspection this is highly suggestive of active halogen chemistry as the reaction rate of benzene with Cl atoms is 21 times slower than that of acetylene with Cl. Also benzene hardly even reacts with Br atoms whilst acetylene will also react quickly with this species (Table 4). CO reacts with OH but not with Cl or Br atoms [2.41×10^{-13} molecule cm^3 s^{-1} (DeMore et al., 1997)].

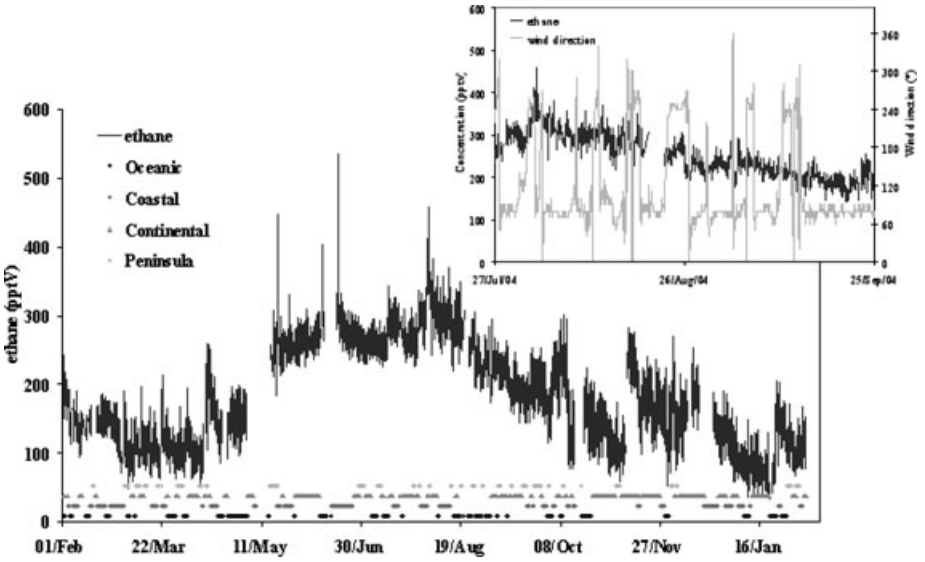

Fig. 6. Time-series of ethane annotated with airmass origin; inset showing ethane and wind direction.

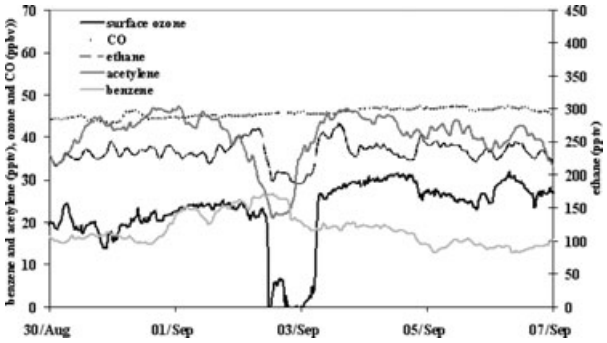

Fig. 7. Surface ozone, CO, ethane, acetylene and benzene time-series for an ozone depletion event on the 2nd–3rd of September.

Following the methodology of Jobson et al., (1994a) who observed similar O_3 depletions in the Arctic, we can take the mean concentration of a hydrocarbon just prior to the depletion as background $[RH]_{BKG}$ and the concentration of the hydrocarbon at the maximum rate of change of the O_3 as $[RH]_{LO}$ and can relate these for each episode using Cl atom reaction kinetics (1) (Table 5):

$$[RH]_{LO} = [RH]_{BKG} \exp\left(-k_{Cl}\int [Cl]dt\right), \quad (1)$$

where k_{Cl} is the Cl atom rate constant for reaction with a given NMHC and [Cl] is the Cl atom concentration integrated over the reaction time t. Plotting ln ($[RH]_{LO}/[RH]_{BKG}$) versus k_{Cl} should give a linear relationship with a gradient equal to $-\int$ [Cl]dt, the integrated Cl concentration.

The results are detailed in Table 6. For the 2nd of September event, this analysis gives a slope of –2.93 (± 0.09) × 10^9 atom cm^{-3} s (Fig. 8). To calculate the extent of O_3 removal by reaction with Cl atoms at this time, we can use the same equation as above (1) but substituting O_3 instead of hydrocarbons, together with k_{Cl+O3} as k_{Cl} (2) (rate constants, Table 3) and slope $= -\int$ [Cl] dt:

$$[O_3]_{LO} = [O_3]_{BKG} \exp(-k_{Cl}\int [Cl]dt). \quad (2)$$

Based on the magnitude of hydrocarbon depletion, this equates to an O_3 removal of only 2.9% by Cl so significant other removal mechanisms must be occurring to make this up to 100% (from 23 to 0 ppbv). If we assume that the reaction time within our airmass resulting in NMHC depletion is bounded between 1 and 20 d (86 400 and 1 728 000 s), then the average [Cl] for this period can be constrained to be between 1.7 × 10^3 and 3.4 × 10^4 atom cm^{-3}, slightly lower than previous indirect measurements of between 3.9 × 10^3 and 7.7 × 10^4 atom cm^{-3} (Jobson et al., 1994a).

During this episode, however, acetylene and ethene also showed some deviation from the predicted Cl kinetics line – both compounds were depleted by more than their rate constant with Cl atoms would suggest (Fig. 8). This may be postulated to be due to an additional removal by Br atoms as these hydrocarbons also react with Br via addition reactions, whereas this is not the case for the other species (Table 4, rate constants). The concentration of Br atoms at this time can then be calculated by using the following equation (3) (where k_{Br} is $k_{Br+acetylene}$):

$$-k_{Br}\int [Br]dt = \ln([C_2H_2]_{LO}/[C_2H_2]_{BKG})_{observed} - \ln([C_2H_2]_{LO}/[C_2H_2]_{BKG})_{Cl\,atom}, \quad (3)$$

which gives a value of $-k_{Br}\int$ [Br]dt of –0.56. Repeating this analysis for ethene gives a value of –1.45. $-\int$ [Br]dt is therefore equal to –1.4 (± –0.07) × 10^{13} and –2.1 (± –0.04) × 10^{12} atom cm^{-3} s, using acetylene and ethene, respectively (Table 4, rate constants), giving an average of –8.3 × 10^{12} atom cm^{-3} s.

Whereas the changes in NMHC due to Cl reactions were calculated from regression values, $-\int$ [Br]dt uses the Br + acetylene

Table 4. Calculated rate constants for austral spring (August–September) T = 243 K, Pressure = 980 hPa using IUPAC Evaluated Kinetic data – March 2005 (http://www.iupac-kinetic.ch.cam.ac.uk/)

	C_2H_6	C_3H_8	*iso*-C_4H_{10}	*n*-C_4H_{10}	C_2H_2	C_2H_4	C_6H_6	O_3
OH ($\times 10^{-12}$ cm^3 molecule^{-1} s^{-1})	0.12	0.73	1.85	1.85	7.67	8.22	1.06	–
Cl ($\times 10^{-10}$cm^3 molecule^{-1} s^{-1})	0.55	1.41	1.43	2.18	0.84	0.93	0.04	0.79
Br ($\times 10^{-13}$ cm^3 molecule^{-1} s^{-1})	–	–	–	–	0.39	7.04	–	0.66

Table 5. Background $[RH]_{BKG}$ and minimum $[RH]_{LO}$ mixing ratios for selected NMHC (and O_3) during the O_3 depletion event on the 2nd September and also during the spring depletion

Species	02/09/04 $[HC]_{BKG}$	03/09/04 $[HC]_{LO}$	ln($[HC]_{LO}$/ $[HC]_{BKG}$)	22/08/04 $[HC]_{BKG}$	09/09/04 $[HC]_{LO}$	ln($[HC]_{LO}$/ $[HC]_{BKG}$)
Ethane	254.8	204.7	–0.219	240.6	215.0	0.112
Ethene	32.1	5.8	–1.718	–	–	–
Propane	48.4	33.8	–0.357	46.9	35.1	0.290
Iso-butane	7.5	3.6	–0.730	3.8	3.6	0.047
N-butane	8.1	4.1	–0.670	6.4	7.7	–0.188
Acetylene	40.5	18.0	–0.810	35.7	34.9	0.022
Benzene	25.2	23.1	–0.086	32.2	17.6	0.603
Ozone	23.0	0	–	–	–	–

Values for NMHC in pptv and O_3 in ppbv.

(or ethene) rate constant directly and is therefore sensitive to the temperature dependence of the Br + acetylene (or ethene) rate constant. Over the range 233–253 K, the average value calculated for $-\int [Br]dt$ varies by $\pm 0.63 \times 10^{12}$ atom cm^{-3} s. Using the ozone data for the period in question, however, it is possible to estimate, as a percentage, the extent to which Br reactions occur (4) (k_{Br} is now k_{Br+O3}, Table 4):

$$\frac{[O_3]_t}{[O_3]_0} = \exp\left(-k_{Br+O3}\int [Br]dt\right). \quad (4)$$

This gives an average O_3 loss by reaction with Br of 99.5 ($\pm$ 0.2)% (error over the temperature range 233–253 K). Assuming that the reaction time within the airmass is once again between 1 and 20 d, the mean [Br] is bounded by values of 4.8×10^6 and 9.6×10^7 atom cm^{-3}. This is up to 1000 times higher than the value for the Cl.

Comparing the observed values of O_3 ($[O_3]_{LO}$ from Table 6) to the calculated values based on Br and Cl removal estimated from NMHC behaviour, it is clear that there is significant halogen chemistry causing these short-term perturbations.

Previous work has also shown this to be true during the equivalent seasonal period in the Arctic, where it is thought to be dominated by Br chemistry rather than Cl chemistry (Jobson et al., 1994a; Evans et al., 2003). Br atom production has been attributed to result from heterogeneous reactions such as,

$$BrO + HO_2 \rightarrow HOBr + O_2. \quad (R.1)$$

$$HOBr + Br^-_{aq} + H_{aq} \rightarrow Br_2 + H_2O_{aq}, \quad (R.2)$$

$$Br_2 + h\upsilon \rightarrow 2Br(\lambda < 600nm). \quad (R.3)$$

Originally these reactions were thought to be mainly occurring on the surface of sea salt particles (Vogt et al., 1996). In recent years, however, the surface of frost flowers, associated with newly forming sea-ice, has been highlighted as a perfect environment (e.g. highly saline, large surface area), for the autocatalytic oxidation of sea salt halides, specifically bromide, resulting in 'Br explosion events' (Platt and Hönninger, 2003). These events become more significant under conditions of strong inversion layers in which surface emissions are confined to the boundary layer and there is little mixing with the free troposphere (Rankin and Wolff, 2003). During the Arctic studies Evans et al., (2003) suggested that specifically Cl atom chemistry was only important during the early stages of depletion, while Br chemistry remains active even as O_3 drops below 1 ppbv (Jobson et al., 1994a).

4.4.2. Springtime alkane decrease. Ethane and propane data illustrate that in this study there was an earlier decrease in concentrations in austral spring away from the OH-dependent sinusoidal seasonal cycle than in the previously published atmospheric data sets (Rudolph et al., 1989; Rudolph, 1995; Clarkson et al., 1997). The wind direction remained constant during this period (inset plot in Fig. 6) and assuming production by photolysis of O_3 only, it is likely that there was insufficient OH produced during August to consistently reduce the concentrations of all the NMHCs to the observed extent. For example, ethane and propane decreased by 25.6 and 11.8 pptv, respectively, between the 22nd of August and 8th of September and this would require a constant average [OH] of 2.05×10^5 molecule cm^{-3}. This value

Table 6. Calculated values for time-integrated Cl and Br for the depletion event together with the observed O_3 destruction for this period. Also the calculated values for time-integrated Cl during spring

Period of analysis	$\int$ [Cl] dt (molecules cm^{-3} s)	[Cl]: 20 d–1 d (molecules cm^{-3})	[Br]:20 d–1 d (molecules cm^{-3})	$[O_3]_{LO\ calculated}$ (ppbv)	$[O_3]_{LO\ observed}$ (ppbv)
2/9/04–4/9/04	2.93 ($\pm$ 0.094) $\times$ 10^9	1.70 $\times$ 10^3–3.39 $\times$ 10^4	4.79 $\times$ 10^6–9.58 $\times$ 10^7	–2.4	0
22/08/04–08/09/04	2.92 ($\pm$ 0.112) $\times$ 10^9	1.69 $\times$ 10^3–3.38 $\times$ 10^4	–	–	–

for spring is however higher than measurements made even in February (austral summer) at Palmer Station, Antarctica of 1.1 $\times$ 10^5 molecule cm^{-3} (Jefferson et al., 1998). More recently higher [OH] (average 2 $\times$ 10^6 molecules cm^{-3}) have been observed at the South Pole in summer but these are thought to be due to elevated [NO] emitted from the snow pack under 24-h sun conditions (Davis et al., 2001; Mauldin et al., 2001).

The rapid rate of reaction of ethane and propane with chlorine, however (up to 100 times faster than that with OH), leads to the conclusion that this may be the more likely additional oxidant for these species over this period (Table 4). The previous short-term O_3 depletion events clearly showed the presence of Cl atoms as a contributor in inducing NMHC variability on the hour–day time-scale (albeit small compared to Br), so in this section we aim to demonstrate the presence and effect of Cl as a cause of day-to-week time-scale variability.

Iso-butane and *n*-butane have almost identical reaction rates (and hence lifetime) with respect to OH, whilst the reaction of *n*-butane with Cl atoms proceeds almost twice as fast as the reaction of Cl atoms with its isomeric partner (Table 4). The examination of *iso*-butane/*n*-butane versus *n*-butane therefore will indicate the dominant radical chemistry acting on that airmass. A constant *iso*-/*n*- ratio independent of abundance implies OH-only chemistry. Including a third compound, in this case propane, eliminates analytical bias from atmospheric dilution and mixing, and a simultaneous constant *iso*-butane/propane ratio assures the Cl influence. Each data point in Fig. 9 is a daily average and shows that at least for the August–September data, the *iso*-/*n*- ratio varies between 0.42 and 1.55, whilst the *iso*-butane/propane ratio remains at between 0.14 and 0.55. These data had average 1σ standard deviations of 0.11 on the *x*-axis (*iso*-butane/propane) and 0.45 on the *y*-axis (*iso*-butane/*n*-butane). This relationship for the month-long period indicates the presence of significant Cl and shows that this is acting on relatively long temporal scales. There was also evidence of a similar occurrence in April–May moving through into polar night, as the *iso*-/*n*- ratio varied between 0.63 and 1.34, whilst the *iso*-butane/propane ratio remained between 0.19 and 0.41 (except for one outlying point at 0.75, 0.42).

Other evidence for this hypothesis can be obtained by comparing the behaviour of CO with ethane and O_3 for the spring period (Fig. 10). CO is removed from the atmosphere only by its reaction with OH [2.41 $\times$ 10^{-13} molecule^{-1} cm^3 s^{-1} (DeMore et al., 1997)], whereas O_3 and ethane have reaction rates in August of 9.9 $\times$ 10^{-12} and 5.5 $\times$ 10^{-11} molecule^{-1} cm^3 s^{-1}, respectively, with Cl. In contrast to the decreasing O_3 and ethane levels, the CO concentrations remain high well into the month of September with a peak of 54.0 ppbV for this species occurring on the 10th of September 2005.

By carrying out a similar analysis on the [NMHC] variations to that performed for the short O_3 depletion event periods but over longer time-scales, a [Cl] can be estimated which if present, would cause the observed decrease and deviation for ethane and propane from the sinusoidal fit.

Table 7. Average summer and winter values for NMHC and calculated lifetimes based on summer average OH = 3×10^5 molecules cm^{-3} (Lee and Bloss, private communication) and winter [OH] = 1×10^5 molecules cm^{-3} (Bloss et al. 2005)

Compound	Summer (December–February) ~1375 samples (pptv)	Lifetime (d)	Winter (June–August) ~1492 samples (pptv)	Lifetime (d)	Whole campaign ~5780 samples (pptv)
Ethane	125.6 ± 38.8	236.7	275.9 ± 32.8	890.3	184.8 ± 73.8
Ethene	15.3 ± 18.3	4.7	17.1 ± 18.3	14.1	18.0 ± 19.5
Propane	15.8 ± 13.8	44.6	49.4 ± 18.0	152.5	31.0 ± 21.3
Propene	10.1 ± 32.3	1.3	9.3 ± 11.0	4.0	10.3 ± 20.3
Acetylene	1.0 ± 7.2	5.2	41.9 ± 13.7	15.2	18.5 ± 21.3
iso-butane	0.7 ± 3.2[a]	20.3	7.8 ± 6.5	65.0	3.2 ± 7.2
n-butane	1.0 ± 4.6[a]	18.8	12.5 ± 7.0	61.2	4.9 ± 17.2
Benzene	1.5 ± 5.5[a]	34.5	17.6 ± 9.4	107.2	11.5 ± 14.9

[a]Below detection limit.

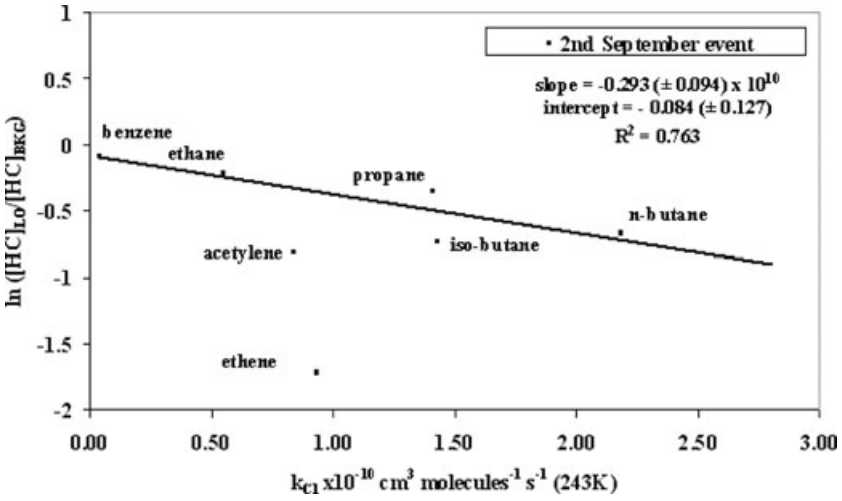

Fig. 8. Correlation between the concentration changes in NMHC during the 2nd September low-ozone episode against their rate of reaction with chlorine atoms. Trend line passes only through benzene, ethane, propane, *iso*-butane and *n*-butane.

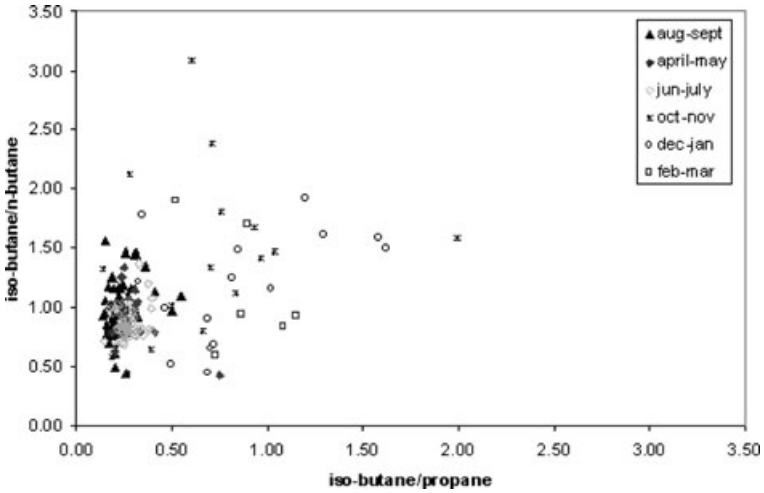

Fig. 9. A plot of *iso*-/*n*-butane against *iso*-butane/propane for the year, divided bimonthly. The varying *iso*-/*n*-butane ratio indicates chlorine chemistry using a third compound to remove dilution effects.

The results for this spring analysis (22nd of August–8th of September 2004) are illustrated in Fig. 11 and detailed in Table 6. Using the slope of –2.73 (± 0.116) × 10^9 atom cm^{-3} s and assuming that the reaction time within our airmass resulting in NMHC depletion is 14 d (1 209 600 s) then this gives an average [Cl] of 2.26 × 10^3 atom cm^{-3}.

In order to rule out the influence of OH chemistry at this time, a similar process (Fig. 12) was applied to the reaction

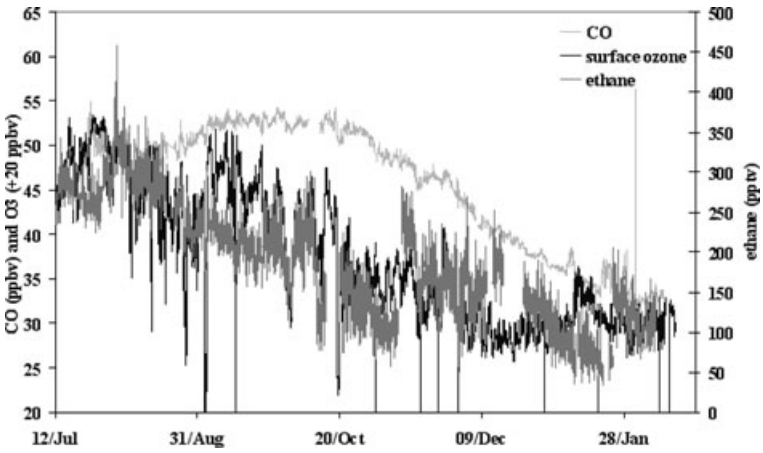

Fig. 10. Time-series of carbon monoxide, surface ozone and ethane for the austral spring–summer period.

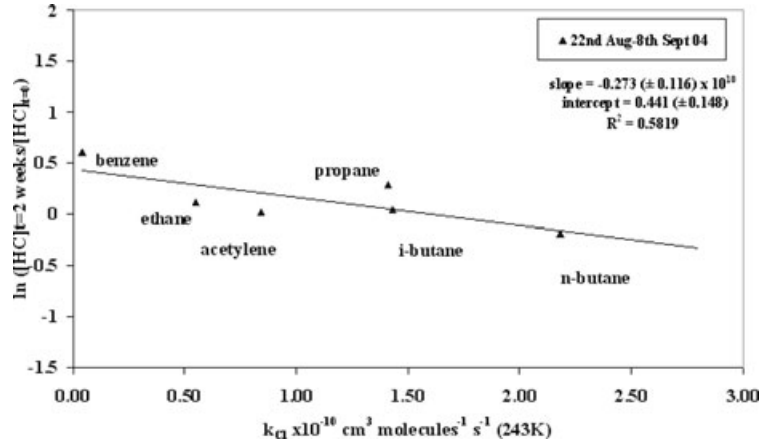

Fig. 11. Correlation between the concentration changes in NMHC during a period in austral spring against their rate of reaction with chlorine atoms.

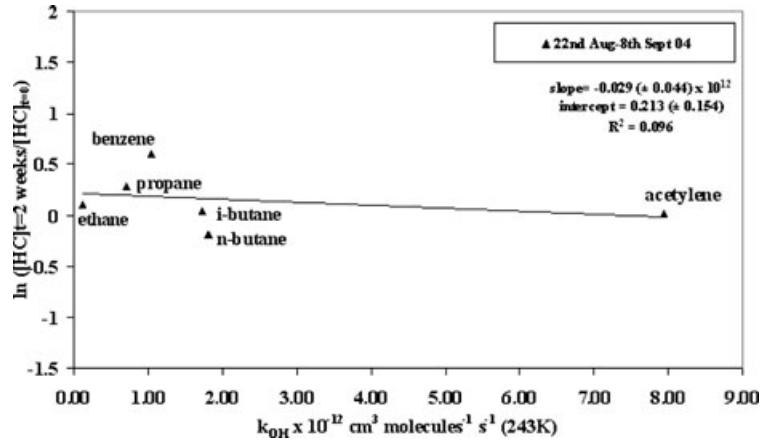

Fig. 12. Correlation between the concentration changes in NMHC during a period in austral spring against their rate of reaction with OH radicals.

of NMHCs with OH. The results showed very little correlation providing further assurance that the NMHC behaviour during this time related to Cl atom kinetics rather than that of OH radicals.

In addition, this entire analysis was performed not only for the time period in question but also for other periods during the year in order to determine that the presence of significant Cl atoms was a feature unique to this time period. R^2 fit values were calculated based on the reactions of the NMHC with both Cl atoms and OH radicals [using the plots of ln $([RH]_{LO}/[RH]_{BKG})$ versus k_{Cl} or versus k_{OH} respectively], over two week periods that satisfied the following conditions.

(i) Greater than three NMHC species present above the detection limit, and

(ii) negative correlation within the plot.

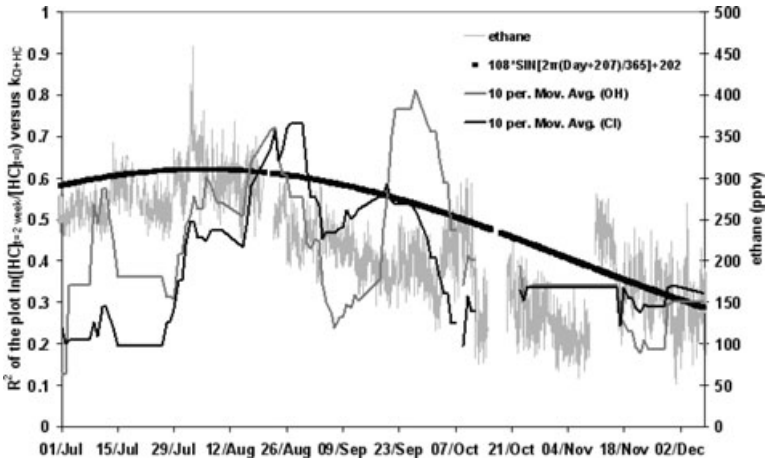

Fig. 13. A graph to show the variation in R^2 of a plot of 'change in NMHC over 2 weeks against their reaction rate with chlorine atoms or OH radicals' (e.g. Figs. 11 and 12) as a function of time of year. No attempt is made to accurately quantify the relative contributions from OH and Cl but instead to illustrate the dominant chemistry. The time-series for ethane is also plotted together with the predicted sinusoidal fit.

The R^2 fit values were plotted as a function of time and highlighted as a dominance of Cl chemistry over that of OH between August and September 2004 (Fig. 13).

At present there is no method sensitive enough to measure the halogen atomic species at levels of 10^3–10^4 atom cm^{-3}; however, indirect evidence obtained from model calculations and laboratory studies continues to suggest their potential importance in the regional tropospheric chemistry of areas such as the Antarctic (Pszenny et al., 1993; Rudolph et al., 1996). Previous studies have instead chosen to focus on either making measurements of their precursors (Pszenny et al., 1993; Khalil and Rasmussen, 1999a, 1999b) or, as in this study, have used measurements and behaviour of other chemical species to infer in some cases the presence of the atomic species, and in others their potential atmospheric concentrations. Hopkins et al., (2002), who reported NMHC results obtained from a ship platform in the Arctic, observed that significant halogen chemistry was evident during measurements at high latitudes, a conclusion resulting from observations of changes in *iso*- and *n*-butane ratios (as discussed previously in this section). Other studies focusing on specific events, such as O_3 depletion to calculate the concentrations for that short time period, found similar concentrations to those seen here (Jobson et al., 1994a; Ariya et al., 1999). Work performed by Rudolph et al., (1996), who used the global budgets of ethane and tetrachloroethene to calculate a global tropospheric budget for Cl atoms resulted in the reporting of values for [Cl] of 1×10^3 and 2×10^3 atom cm^{-3} in the Northern Hemisphere and Southern Hemisphere, respectively. As the maximum values for this Antarctic region are expected to occur in late winter/early spring, the estimated concentration of 2.3×10^3 atom cm^{-3} for [Cl] over this spring period is in line with the results reported in that particular study.

Reactive halogen species such as Cl atoms are produced from the photolysis of less-stable precursors including methyl halides, polyhalogenated species and from species such as XNO or XNO_2 (where X = Cl or Br) formed from sea-salt aerosol. In the Antarctica, the chloride in sea-salt particles depletes in summer consistent with the loss of HCl during the reaction with gaseous acidic species. During the winter, however, chloride in sea-salt particles is enhanced as a result of fractionation which occurs as new sea ice forms. Methyl halides have a source in the ocean (Carpenter et al., 1999; Khalil et al., 1999) and are also produced from biomass burning in the tropics (Blake et al., 1996). The oceans can also be a sink for organic halogenated species such as bromoform (Quack et al., 2003). In addition, methyl chloride, chloroform, dichloromethane, perchloroethylene and trichloroethylene are products of industry and although exist mainly in the Northern Hemisphere, can be transported and degraded in the troposphere to release atomic halogens (Khalil and Rasmussen, 1999b). Measurements of methyl chloride and chloroform made in the Antarctica between 1981 and 1997 illustrate seasonal trends in concentrations for these species with similar maxima of around 20 pptV (6×10^8 molecule cm^{-3}) occurring in August–September (Khalil and Rasmussen, 1999a; 1999b).

4.5. Ethene and propene seasonal variation

During CHABLIS, ethene and propene were generally at very low levels and showed a large variability typical of short-lived species. As discussed within the Experimental Section (Section 3), although relative errors become large at low concentrations and tend towards 100%, the absolute errors remain low. For example, where the noise is equivalent to a concentration of 3 pptV a peak with S/N ratio of 1:1 must have a concentration ranging between 0 and 6 pptv and hence a relative error of 100%. Average values for the campaign were 18 ± 20 pptV for ethene and 10 ± 20 pptV for propene and these were calculated using the actual measured values even if the measurements fell below the detection limits of 4 and 3 pptV for ethene and propene, respectively.

There are generally few reported measurements of ethene and propene in Antarctica but it is unclear whether this is due to there being none present in other studies or whether the past methods used to measure them were unsatisfactory (e.g. unstable

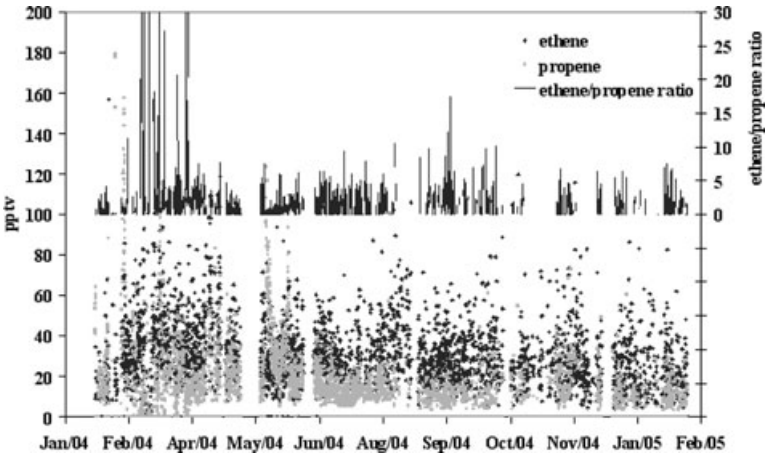

Fig. 14. Time-series of ethene, propene and ethene/propene.

canister samples) (Donahue and Prinn, 1990; Gros et al., 1998). High values for ethene and propene were reported from measurements at Amsterdam Island in the Southern Hemisphere but these are perhaps unique to this island location and unlikely to be comparable to observations in Polar Regions (Bonsang et al., 1990).

Ethene/propene ratios calculated for the campaign were found to have an annual average of 1.9 ± 7 which although similar to that of 1.7 ± 0.3 collected from canister samples at Neumayer (Rudolph et al., 1989), has a variance over three times its value (Fig. 14). Published estimates for oceanic emissions (0.9–2.1 ethene/propene on a volume per volume basis) are in agreement with the ratios observed for the majority of this year-round study and there is clear evidence of a seasonal cycle in the monthly average plot of the data set (Fig. 15). Similar to this study, previous measurements have shown that a maximum in these species concentrations has been observed in austral autumn corresponding to a minimum in sea-ice and therefore when sea-air flux is at a maximum (Rudolph et al., 1989; Wagenbach et al., 1988). However, the average value for ethene at this coastal site is four times lower than the average 74 pptV measured at the South Pole between 1979 and 1985 which in isolation would imply that there is actually less influence from oceanic production at Halley than at the South Pole (Khalil and Rasmussen, 1986). Although highly variable, the above background values for these alkene species throughout the winter indicate some influence from long-range transport due to the alkenes' extended lifetime (14.1 d for ethene and 4 d for propene) (Table 7) ([OH] = 1×10^5 molecules cm^{-3} at the rate of 250 K, Bloss et al., 2005), rate constants from http://mcm.leeds.ac.uk/MCM/home.http (Jenkin et al. 2003), and a strong possibility also exists of a source from the snow pack similar to observations in the Arctic troposphere (Bottenheim et al., 2002a; Swanson et al., 2002). The deeper boundary layer at Halley compared to the South Pole could explain the lower concentrations observed at Halley, if the snow pack is the source.

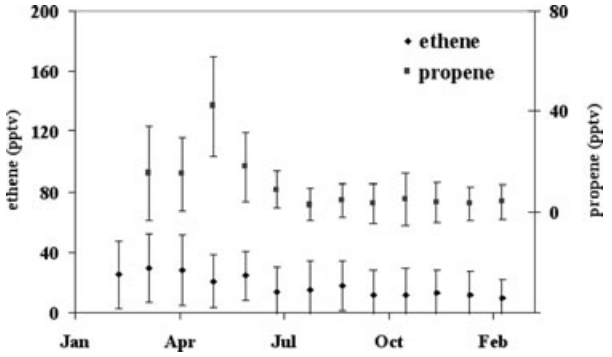

Fig. 15. Monthly average cycle of ethene and propene.

5. Conclusions

A year-long continuous data set of C_2–C_8 NMHCs *in situ* measurements at Halley, Antarctica has determined both the seasonal trends and the smaller-scale variability of these species in the Antarctic Boundary Layer. An OH-dependent sinusoidal pattern was evident in the alkane measurements and the magnitude of the data was found to be in good agreement with previous work carried out in this region of the atmosphere. Main deviations from this trend occurred as a result of large-scale airmass changes to the site, although due to the long period that had elapsed since emissions it was impossible to allocate specific source regions for the species measured. The behaviour of NMHCs during O_3 depletion episodes provided some insight into the presence of other oxidants such as Cl and Br atoms at these times, similar to work performed in the Arctic. In addition, rapidly decreasing alkane concentrations in Spring leading to further deviation away from the typical OH-driven trend implied a more consistent influence from these oxidants and evidence was presented for a persistent [Cl] of around 2.3×10^3 atom cm^{-3} in line with average global estimates for this atomic species. Although demonstrating some seasonal dependence with oceanic

emissions, significant ethene and propene concentrations at Halley also implied the existence of a snow pack source in summer. In addition, lower absolute values when compared to those seen at the South Pole were in line with the deeper boundary layer at Halley.

The frequency and continuous nature of this NMHC data set has facilitated investigation into the levels of oxidant activity and the relative importance of oxidants such as the halogen atoms during times of low OH. It is clear that NMHCs are extremely good proxies for many such oxidants, and this data set, in addition to those of the other species measured during CHABLIS, contributes to the understanding of their detailed interactions under extreme conditions and also within a pristine environment. This information is essential if we are to be able to successfully model the global atmosphere.

6. Acknowledgments

The authors acknowledge that this work would not have been possible without logistical and scientific support from the British Antarctic Survey. Thanks to the principal investigators and instrumental scientists for all their hard work throughout the project and to the Natural Environment Research Council Antarctic Funding Initiative who funded the CHABLIS programme under grant number NER/G/S/2001/00558.

References

Andreae, M. O. and Merlet, P. 2001. Emission of trace gases and aerosols from biomass burning. *Global Biogeochem. Cycles* **15**, 955–966.

Ariya, P. A., Niki, H., Harris, G. W., Anlauf, K. G. and Worthy, D. E. J. 1999. Polar sunrise experiment 1995: hydrocarbon measurements and tropospheric Cl and Br-atoms chemistry. *Atmos. Environ.* **33**, 931–938.

Blake, N. J., Blake, D. R., Sive, B. C., Chen, T. Y., Rowland, F. S. and co-authors. 1996. Biomass burning emissions and vertical distribution of atmospheric methyl halides and other reduced carbon gases in the South Atlantic region. *J. Geophys. Res.* **101**, 24 151–24 164.

Bloss, W. J., Evans, M. J., Lee, J. D., Sommariva, R., Heard, D. E. and co-authors. 2005. The oxidative capacity of the troposphere: Coupling of field measurements of OH and a global chemistry transport model. *Faraday Discuss.* **130**, 425–436.

Bonsang, B., Kanakidou, M. and Lambert, G. 1990. NMHC in the marine atmosphere: Preliminary results of monitoring at Amsterdam Island. *J. Atmos. Chem.* **11**, 169–178.

Bottenheim, J. W., Boudries, H., Brickell, P. C. and Atlas, E. 2002a. Alkenes in the Arctic boundary layer at Alert, Nunavut, Canada. *Atmos. Environ.* **36**, 2585–2594.

Bottenheim, J. W., Dibb, J. E., Honrath, R. E. and Shepson, P. B. 2002b. An introduction to the ALERT 2000 and SUMMIT 2000 Arctic research studies. *Atmos. Environ.* **36**, 2467–2469.

Carpenter, L. J., Sturges, W. T., Penkett, S. A., Liss, P. S., Alicke, B. and co-authors. 1999. Short-lived alkyl iodides and bromides at Mace Head, Ireland: Links to biogenic sources and halogen oxide production. *J. Geophys. Res.* **104**, 1679–1689.

Clarkson, T. S., Martin, R. J. and Rudolph, J.. 1997. Ethane and propane in the southern marine troposphere. *Atmos. Environ.* **31**, 3763–3771.

Davis, D., Nowak, J. B., Chen, G., Buhr, M., Arimoto, R. and co-authors. 2001. Unexpected high levels of NO observed at South Pole. *Geophys. Res. Letts.* **28**, 3625–3628.

DeMore, W. B., Sander, S. P., Golden, D. M., Hampson, R. F., Kurylo, M. J. and co-authors. 1997. *Chemical kinetics and photochemical data for use in stratospheric modelling, evaluation number 12* JPL Publications, Pasadena, California.

Dominé, F. and Shepson, P. B.. 2002. Air-snow interactions and atmospheric chemistry. *Science* **297**, 1506–1510.

Donahue, N. M. and Prinn, R. G. 1990. Nonmethane hydrocarbon chemistry in the remote marine boundary layer. *J. Geophys. Res.* **95**, 18 387–18 411.

Durana, N., Navazo, M., Gomez, M. C., Alonso, L., Garcia, J. A. and co-authors. 2006. Long term hourly measurement of 62 non-methane hydrocarbons in an urban area: Main results and contribution of non-traffic sources. *Atmos. Environ.* **40**(D16), 2860–2872.

ECMWF. The description of the ECMWF/WRCP Level III-A global atmospheric data archive. ECMWF. 1995. Reading, RG2 9AX, UK, Shinfield Park.

Evans, M. J., Jacob, D. J., Atlas, E., Cantrell, C. A., Eisele, F. and co-authors. 2003. Coupled evolution of BrOx-ClOx-HOx-NOx chemistry during bromine-catalyzed ozone depletion events in the arctic boundary layer. *J. Geophys. Res.* **108**, art. no.-8368.

Fischer, R., Weller, R., Jacobi, H. W. and Ballschmiter, K. 2002. Levels and pattern of volatile organic nitrates and halocarbons in the air at Neumayer Station (70 degrees S), Antarctic. *Chemosphere* **48**, 981–992.

Goldstein, A. H., Wofsy, S. C. and Spivakovsky, C. M. 1995. Seasonal variations of nonmethane hydrocarbons in rural New England: Constraints on OH concentrations in northern midlatitudes. *J. Geophys. Res.,* **100**, D10, 21 023–21 033.

Gros, V., Martin, D., Poisson, N., Kanakidou, M., Bonsang, B. and co-authors. 1998. Ozone and C_2–C_5 hydrocarbon observations in the marine boundary layer between 45°S and 77°S. *Tellus* **50B**, 430–448.

Hopkins, J. R., Jones, I. D., Lewis, A. C., McQuaid, J. B. and Seakins, P. W. 2002. Non-methane hydrocarbons in the Arctic boundary layer. *Atmos. Environ.* **36**, 3217–3229.

Hopkins, J. R., Lewis, A. C. and Seakins, P. W. 2005. Analysis and applications of measurements of source dominated hydrocarbon concentrations from the PUMA campaigns in June/July 1999 and January/February 2000 at an urban background site in Birmingham, UK. *Atmos. Environ.* **39**, 535–548.

Jacobi, H.-W., Weller, R., Jones, A. E., Anderson, P. S. and Schrems, O. 2000. Peroxyacetyl nitrate (PAN) concentrations in the Antarctic troposphere measured during the Photochemical Experiment at Neumayer (PEAN'99). *Atmos. Environ.* **34**, 5235–5247.

Jacobi, H.-W., Frey, M. M., Hutterli, M. A., Bales, R. C., Schrems, O. and co-authors. 2002. Measurements of hydrogen peroxide and formaldehyde exchange between the atmosphere and surface snow at Summit, Greenland. *Atmos. Environ.* **36**, 2619–2628.

Jenkin, M. E., Saunders, S. M., Wagner, V. and Pilling, M. J. 2003. Protocol for the development of the Master Chemical Mechanism, MCM v3 (Part B): tropospheric degradation of aromatic volatile organic compounds. *Atmos. Chem. Phys.* **3**, 181–193.

Jobson, B. T., Niki, H., Yokouchi, Y., Bottenheim, J., Hopper, F. and co-authors. 1994a. Measurements of C_2-C_6 hydrocarbons during the Polar Sunrise 1992 Experiment: Evidence for Cl atom and Br atom chemistry. *J. Geophys. Res.* **99**, 25 355–25 368.

Jobson, B. T., Wu, Z., Niki, H. and Barrie, L. A. 1994b. Seasonal trends of isoprene, C_2-C_5 alkanes, and acetylene at a remote boreal site in Canada. *J. Geophys. Res.* **99**(D1), 1589–1599.

Jones, A. E., Weller, R., Wolff, E. W. and Jacobi, H. W. 2000. Speciation and rate of photochemical NO and NO_2 production in Antarctic snow. *Geophys. Res. Letts.* **27**, 345–348.

Jones, A. E., Anderson, P. S., Wolff, E. W., Turner, J., Rankin, A. M. and co-authors. 2006. A role for newly forming sea ice in springtime polar tropospheric ozone loss? Observational evidence from Halley station, Antarctica. *J. Geophys. Res.* **111**, D08306, doi:10.1029/2005JD006566.

Kanakidou, M., Bonsang, B., Roulley, J. C. L., Lambert, G., Martin, D. and co-authors. 1988. Marine source of atmospheric acetylene. *Nature* **333**, 51–52.

Kanakidou, M., Singh, H. B., Valentin, K. M. and Crutzen, P. J. 1991. A two-dimensional study of ethane and propane oxidation in the troposphere. *J. Geophys. Res.* **96**(D8), 15 395–15 413.

Kaspers, K. A., van de Wal, R. S. W., de Gouw, J. A., Hofstede, C. M., van den Broeke, M. R. and co-authors. 2004. Analyses of firn gas samples from Dronning Maud Land, Antarctica: Study of nonmethane hydrocarbons and methyl chloride. *J. Geophys. Res.* **109**, art. no.-D02307.

Khalil, M. A. K., Moore, R. M., Harper, D. B., Lobert, J. M., Erickson, D. J. and co-authors. 1999. Natural emissions of chlorine-containing gases: Reactive Chlorine Emissions Inventory. *J. Geophys. Res.* **104**, 8333–8346.

Khalil, M. A. K. and Rasmussen, R. A. 1986. Temporal variability of C_2-hydrocarbons at the South Pole: Seasonal cycles and the possible effects of El-Nino. *Antarct. J. U.S.* **21**, 244–245.

Khalil, M. A. K. and Rasmussen, R. A. 1999a. Atmospheric chloroform. *Atmos. Environ.* **33**, 1151–1158.

Khalil, M. A. K. and Rasmussen, R. A. 1999b. Atmospheric methyl chloride. *Atmos. Environ.* **33**, 1305–1321.

Kottmeier, C. and Fay, B. 1998. Trajectories in the Antarctic lower troposphere. *J. Geophys. Res.* **103**, 10 947–10 959.

Lewis, A. C., Carpenter, L. J. and Pilling, M. J. 2001. Nonmethane hydrocarbons in Southern Ocean boundary layer air.. *J. Geophys. Res.* **106**, 4987–4994.

Mauldin, R. L., Eisele, F. L., Tanner, D. J., Kosciuch, E., Shetter, R. and co-authors. 2001. Measurements of OH, H2SO4, and MSA at the South Pole during ISCAT. *Geophys. Res. Letts.* **28**, 3629–3632.

Murayama, S., Nakasawa, T., Tanaka, M., Aoki, S. and Kawaguchi, S. 1992. Variations of tropospheric ozone mixing ratio over Syowa Station, Antarctica. *Tellus* **44B**, 262–272.

Platt, U. and Hönninger, G. 2003. The role of halogen species in the troposphere. *Chemosphere* **52**, 325–338.

PORG. Ozone in the United Kingdom 1993. *Third report of the U.K. photochemical oxidants review group: 1993*. Department of the Environment, London.

Pszenny, A. A. P., Keene, W. C., Jacob, D. J., Fan, S., Maben, J. R. and co-authors. 1993. Evidence of inorganic chlorine gases other than hydrogen chloride in marine surface air. *J. Geophys. Res.* **20**, 699.

Quack, B. and Wallace, D. W. R. 2003. Air-sea flux of bromoform: Controls, rates and implications. *Global Biogeochem. Cycles* **17**(1), Art. No. 1023.

Rankin, A. M. and Wolff, E. W. 2003. A year-long record of size-segregated aerosol composition at Halley, Antarctica. *J. Geophys. Res.* **108**, art. no.-4775.

Ratte, M., Bujok, O., Spitzy, A. and Rudolph, J. 1998. Photochemical alkene formation in seawater from dissolved organic carbon: Results from laboratory experiments. *J. Geophys. Res.* **103**, 5707–5717.

Riedel, K., Weller, R., Schrems, O. and Konig-Langlo, G. 2000. Variability of tropospheric hydroperoxides at a coastal surface site in Antarctica. *Atmos. Environ.* **34**, 5225–5234.

Royal Society. 1962. *The Royal Society International Geophysical Year Antarctic expedition, Halley Bay 1955-1959*. Brunt.D. Volume III, seismology, meteorology. The Royal Society, London.

Rudolph, J. 1995. The tropospheric distribution and budget of ethane. *J. Geophys. Res.* **100**, 11 369–11 381.

Rudolph, J., Khedim, A., Clarkson, T. and Wagenbach, D. 1992. Long-term measurements of light alkanes and acetylene in the Antarctic troposphere. *Tellus* **44B**, 252–261.

Rudolph, J., Khedim, A. and Wagenbach, D. 1989. The seasonal variation of light non-methane hydrocarbons in the Antarctic troposphere. *J. Geophys. Res.* **94**, 13 039–13 044.

Rudolph, J., Koppmann, R. and PlassDulmer, C. 1996. The budgets of ethane and tetrachloroethene: Is there evidence for an impact of reactions with chlorine atoms in the troposphere?. *Atmos. Environ.* **30**, 1887–1894.

Schnell, R. C., Liu, S. C. and Oltmans, S. J. 1991. Decrease of summer tropospheric ozone concentrations in Antarctica. *Nature*, **351**, 726–729.

Sharma, U. K., Kajii, Y. and Akimoto, H. 2000. Seasonal variation of C_2-C_6 NMHCs at HAPPO, a remote site in Japan. *Atmos. Environ.* **34**, 4447–4458.

Sumner, A. L. and Shepson, P. B. 1999. Snowpack production of formaldehyde and its effect on the Arctic troposphere. *Nature* **398**, 230–233.

Swanson, A. L., Blake, N., Atlas, E., Flocke, F., Blake, D. R. and co-authors. 2003. Seasonal variations of C_1-C_4 nonmethane hydrocarbons and C_1-C_4 alkyl nitrates at the Summit research station in Greenland. *J. Geophys. Res.* **108**, 4065, doi:10.1029/2001JD001445.

Swanson, A. L., Blake, N. J., Dibb, J. E., Albert, M. R., Blake, D. R. and co-authors. 2002. Photochemically induced production of CH_3Br, CH_3I, C_2H_5I, ethene, and propene within surface snow at Summit, Greenland. *Atmos. Environ.* **36**, 2671–2682.

Touaty, M., Bonsang, B., Kanakidou, M. and Poisson, N. 1996. Monitoring and model comparison of the seasonal variation of tropospheric light hydrocarbons at Amsterdam Island. *Proceedings of EUROTRAC Symposium '96*. (Eds.Borrell, P. M., Borrell, P., Cvitas, T., Kelly, K. and Seiler, W.) 613–619.

Vogt, R., Crutzen, P. J. and Sander, R. 1996. A mechanism for halogen release from sea-salt aerosol in the remote marineboundary layer. *Nature* **383**, p. 327–330.

Wagenbach, D., Gorlach, U., Moser, K. and Munnich, K. O. 1988. Coastal Antarctic aerosol:the seasonal pattern of its chemical composition and radionuclide content. *Tellus* **40B**, 426–436.

Wang, J.-L., Chen, W.-L. and Tsai, C.-H. 2000. Cryogen free automated gas chromatography for the measurement of ambient volatile organic compounds. *J. Chromatogr. A* **896**, 31–39.

Wessel, S., Aoki, S., Winkler, P., Weller, R., Herber, A., Gernandt, H. and Schrems, O. 1998. Tropospheric ozone depletion in polar regions - A comparison of observations in the Arctic and Antarctic. *Tellus B* **50**, 34–50.

Wevill, D. J. and Carpenter, L. J. 2004. Automated measurement and calibration of reactive volatile halogenated organic compounds in the atmosphere. *Analyst* v. **129**, 634–638.

Yamamoto, N., Okayasu, H., Hiraiwa, T., Murayama, S., Tuneaki, M. and co-authors. 1998. Continuous determination of volatile organic compounds in the atmosphere by an automated gas chromatographic system.. *J. Chromatogr. A* **819**, 177–186.

Zhou, X., Beine, H. J., Honrath, R. E., Fuentes, J. D., Simpson, W. and co-authors. 2001. Snowpack photochemical production of HONO: A major source of OH in the Arctic boundary layer in springtime.. *Geophys. Res. Lett.* **28**, 4087–4090.